Environmental Research 213 (2022) 113638

Contents lists available at ScienceDirect

Environmental Research

journal homepage: www.elsevier.com/locate/envres

Investigation of the effect of sustainable magnetic treatment on the microbiological communities in drinking water

Xiaoxia Liu [a,b,1], Bernhard Pollner [c,1], Astrid H. Paulitsch-Fuchs [d,e], Elmar C. Fuchs [f,a,*], Nigel P. Dyer [a,g], Willibald Loiskandl [b], Cornelia Lass-Flörl [c]

[a] Wetsus, European Centre of Excellence for Sustainable Water Technology, Oostergoweg 9, 8911 MA Leeuwarden, the Netherlands
[b] Institute of Soil Physics and Rural Water Management, University of Natural Resources and Life Sciences, Vienna, Austria
[c] Division of Hygiene and Medical Microbiology, Medical University of Innsbruck, Innsbruck, Austria
[d] Diagnostic and Research Institute of Hygiene, Microbiology and Environmental Medicine, Medical University of Graz, Neue Stiftingtalstraße 2, 8010, Graz, Austria
[e] Carinthia University of Applied Sciences, Biomedical Science, St. Veiterstraße 47, 9020 Klagenfurt, Austria
[f] Optical Sciences Group, Faculty of Science and Technology (TNW), University of Twente, Drienerlolaan 5, 7522NB Enschede, the Netherlands
[g] Coherent Water Systems, 2 Crich Avenue, DE23 6ES Derby, United Kingdom

ARTICLE INFO

Keywords:
Drinking water
Flowcytometry
magnetic water treatment
microbial community

ABSTRACT

The drinking water scarcity is posing a threat to mankind, hence better water quality management methods are required. Magnetic water treatment, which has been reported to improve aesthetic water quality and reduce scaling problems, can be an important addition to the traditional disinfectant dependent treatment. Despite the extensive market application opportunities, the effect of magnetic fields on (microbial) drinking water communities and subsequently the biostability is still largely unexplored, although the first patent was registered already 1945.

Here flow cytometry was applied to assess the effect of weak magnetic fields (≤10 G) with strong gradients (≈800 G/m) on drinking water microbial communities. Drinking water was collected from the tap and placed inside the magnetic field (treated) and 5 m away from the magnet to avoid any background interferences (control) using both a static set-up and a shaking set-up. Samples were collected during a seven-day period for flow cytometry examination. Additionally, the effects of magnetic fields on the growth of *Pseudomonas aeruginosa* in autoclaved tap water were examined. Based on the fluorescent intensity of the stained nucleic acid content, the microbial cells were grouped into low nucleic acid content (LNA) and high nucleic acid content (HNA). Our results show that the LNA was dominant under nutrient limited condition while the HNA dominates when nutrient is more available. Such behavior of LNA and HNA matches well with the long discussed r/K selection model where r-strategists adapted to eutrophic conditions and K-strategists adapted to oligotrophic conditions. The applied magnetic fields selectively promote the growth of LNA under nutrient rich environment, which indicates a beneficial effect on biostability enhancement. Inhibition on an HNA representative *Pseudomonas aeruginosa* has also been observed. Based on our laboratory observations, we conclude that magnetic field treatment can be a sustainable method for microbial community management with great potential.

1. Introduction

1.1. Magnetic treatment of tap water

The application of (electro-) magnetic fields as a water treatment method in order to suppress the calcium carbonate ($CaCO_3$) deposition on pipe walls has been in use since 1945, when the first commercial application was patented in Belgium (Vermeiren, 1958). Despite the wide applications of magnetic water treatment, a well-accepted explanation of the mechanisms of magnetic field effects on water quality has not been established. So far, most of the studies in the field have focused on the physiochemical aspects of the process and left the microbiological

* Corresponding author. Optical Sciences group, Faculty of Science and Technology (TNW), University of Twente, Drienerlolaan 5, 7522NB Enschede, the Netherlands.
E-mail address: e.c.fuchs@utwente.nl (E.C. Fuchs).
[1] These authors contributed equally to this work.

https://doi.org/10.1016/j.envres.2022.113638
Received 13 May 2022; Accepted 5 June 2022
Available online 12 June 2022

component of water under-investigated (Quinn et al., 1997; Alimi et al., 2009; Lipus et al., 2015).

On the other hand, the effects of magnetic fields on prokaryotes have also been reported in different studies. For instance, inhibitory effects of magnetic fields on the growth rate have been observed on pure culture bacteria such as *Escherichia coli* and *Staphylococcus aureus* (Fojt et al., 2004; Strašák et al., 2002; Masood et al., 2020). In addition, *E. coli* and *Pseudomonas aeruginosa* incubated in medium culture at 37 °C were shown to be more susceptible to antibiotics (kanamycin and amikacin) when exposed to electromagnetic fields (Segatore et al., 2012). Such an inhibitory effect of magnetic fields on microbial growth appears to be very interesting for solving bacteria related problems in drinking water, including planktonic pathogen growth, biofilm formation, or deterioration of aesthetic quality due to secondary metabolites of bacteria. To the knowledge of the authors, there has not yet been a study focusing on the influence of magnetic fields on drinking water microbiology. As a probiotic approach for drinking water quality management has recently attracted attention (Favere et al., 2021; Pinto et al., 2012; Proctor and Hammes, 2015; Van Nevel et al.,2013), a better understanding about the effect of magnetic fields on drinking water microbiology may lead to more sustainable non-invasive methods specifically promoting indigenous communities in drinking water.

1.2. Cytometric fingerprints of microbial communities

The recent advancement of flow cytometric methodologies has allowed real-time measurement of drinking water microbiology, and therefore has opened more possibilities to apply the probiotic approach to drinking water biostability (Props et al., 2018; Van Nevel et al., 2016). Compared to the traditional lengthy culturing methods such as heterotrophic plate count (HPC) (Reasoner and Geldreich, 1985; Allen et al., 2004) that only monitor about 1% of the total microbial species in the drinking water community (Allen et al., 2004)-(Van Nevel et al., 2017), flow cytometry appears to be much more robust and precise as it scans each individual cell to collect information based on its fluorescent signal. Therefore, with this method both quantification and activity status of the entire community can be collected in a couple of hours (Van Nevel et al., 2017; Wang et al., 2010).

Previous literature reports that flow cytometry data generally show a division between two microbial groups in natural water systems based on the nucleic acid content: the so-called “high nucleic acid content” (HNA) microbes and the “low nucleic acid content” (LNA) microbes (Hammes and Egli, 2010; Liu et al., 2017; Šolić et al., 2010). The ratio between HNA and LNA also reflects water sources or contamination events, therefore it can be used as “cytometric fingerprint” to characterize water quality and to monitor the dynamics and structure of microbial communities without the need for taxonomic identification (Besmer et al., 2014; Prest et al., 2013, 2016). In addition, it has also been observed that the two groups of microorganisms differ not only in nucleic acid content, but also in cell size, functionality, and behavior (see Table 1). The HNA cells have been observed to be dominant in nutrient-rich environments and often show a higher growth rate in contaminated drinking water (Liu et al., 2017; Prest et al., 2013; Taguer et al., 2021). In contrast, the LNA cells are often connected to oligotrophic microbes that adapt better in low nutrient environments such as drinking water. LNA cells also rely on different carbon substrates compared to HNA (Liu et al., 2017; Šolić et al., 2010)). Very recently (Favere et al., 2021), the r/K selection theory, which is originally used in macroecology, was applied to microbial ecology of drinking water systems, extensively discussing the possibilities to enrich and manage the so-called “K strategists” to achieve a biologically stable drinking water. According to this concept, the behavior of microorganisms with regard to the nutrient concentration and growth rates can be grouped into two categories, the K-strategists and r strategists. The r-strategists are adapted to a high nutrient availability environment and therefore have a high maximal intrinsic growth rate (μmax) in nutrient rich environment to exploit the nutrients as fast as possible, whereas the K-strategists are adapted to low nutrient availability environments, therefore have higher affinity to nutrients and consequently tend to grow faster when nutrients are scarce. Based on the distinctive behavior of the two groups of microorganisms and their well-matched characteristics with the r/K strategists, we further hypothesized that the HNA microbes employ the r strategy, which means faster growth rate at high nutrient concentration, and LNA microbes employ the K-strategy, which means faster growth rate at low nutrient concentration, as the characteristics of their ecological behavior.

Table 1
Summary of characteristics observed in literature of high nucleic acid content (HNA) microorganisms and low nucleic acid content (LNA) microorganisms.

Characteristics	HNA	LNA	Reference
Size	Big	Small (<0.4 μm or < 0.22 μm)	Proctor et al. (2018)
Functionality	Heterotrophic/ Eutrophic	Oligotrophic	Šolić et al. (2010)
Dominant Habitat	Wastewater, stagnated water, human gut	Low-nutrient environment, drinking water, surface water	(Prest et al., 2013; Taguer et al., 2021)
Growth kinetic in drinking water	Fast in first 3 days (≈1.2 d^{-1})	Slow in first 3 days (≈0.5 d^{-1})	Liu et al. (2017)
Metal interaction	Negatively correlated to metal concentration	Positively correlated to metal concentration	Liu et al. (2017)
Substrate	not correlated with assimilable organic carbon	positively correlated with assimilable organic carbon	Liu et al. (2017)
Exposure to oxidant	Sensitive	Not sensitive	Ramseier et al. (2011)
Taxonomy	e.g. *Pseudomonas* sp., *E. coli*, etc.	e.g. *Parcobacteria*, etc.	(Proctor et al., 2018; Ramseier et al., 2011; Rubbens et al., 2019)
Hypothesized behavior	r-strategy	K-strategy	this paper

1.3. Motivation for the current work

Although magnetic water treatment is widely used globally as an end-of-pipe water softener in people’s homes (Gabrielli et al., 2001), little is known about the effects of the application of magnetic fields on the microbial communities in drinking water, which makes the method controversial. The present work aims to reduce this knowledge gap. In this study, we employed flow cytometry to investigate microbial community dynamics in batch tap water and evaluated the effect of magnetic fields on drinking water microorganisms, both at single species level and community level. We aim to provide a basic understanding of the effect of very weak magnetic fields on drinking water microbiology and explore the possible potential of magnetic water treatment as a sustainable, chemical-free alternative to current treatment methods.

2. Materials & methods

The general experimental workflow can be described as follows: about 500 mL Tap water (native or autoclaved) was collected after 20 min flushing and aliquoted in 16 or 48 glass beakers (100 mL each) from which one half was exposed to weak magnetic fields with strong gradients using water core magnets (WCM) (type DZKL, IPF GmbH, Austria). These magnets show a very weak field strength (<10G) with high magnetic gradients (≈800 G/m) as a special characteristic. They have been used in similar studies before and the magnetic field has been mapped (Sammer et al., 2016; Paulitsch-Fuchs et al., 2021). Maintaining

Table 2
p-values results of Mann-Whitney U tests comparing treated and untreated samples of static set-up experiment.

Days	2	3	4	5	6	7
Total cell	**0.008413***	**0.023628***	**0.000624***	**0.000357***	**0.000264***	**0.004994***
%LNA	**0.006923***	0.181901	0.284608	0.164918	0.804779	0.601006
LNA	**0.027428***	**0.005905***	**0.026902***	**0.005865***	0.124499	**0.003078***
HNA	**0.008901***	**0.014114***	**0.018979***	**0.007198***	0.080064	0.167170

*$p < 0.05$, significant difference (also printed bold).

Table 3
p-values results of Mann-Whitney U tests comparing treated and untreated samples of shaking set-up experiments.

Days	2	3	4	5	6	7	9	11	14
Total cell	0.476878	**0.000001***	**0.019553***	**0.000078***	**0.000005***	**0.000016***	**0.001232***	**0.002121***	**0.408739***
%LNA	**0.02538***	**0.004418***	**0.000372***	**0.000000***	**0.000000***	**0.000002***	**0.000005***	**0.000001***	**0.000018***
LNA	0.878291	**0.000000***	**0.003211***	**0.000002***	**0.000000***	**0.000002***	**0.000001***	**0.000000***	**0.000099***
HNA	0.410241	**0.000030***	0.719416	0.569652	0.190192	0.306295	0.633032	0.549928	0.150537

*$p < 0.05$, significant difference (also printed bold).

a spatial separation of 5 m between experiment- and control-group, both groups were incubated at room temperature (22–23 °C) (Amprobe TR200-A, Fluke Europe BV, the Netherlands) for a number of days ranging from 7 to 28 days (table S2). At regular time intervals and under sterile conditions, samples were taken from each beaker, and the number of microbial cells in each sample as well as their fluorescence distribution were determined using flow cytometry. The date of the experiments and the relevant chemical parameters indicating water qualities can be found in table S1. The experiment was performed in the north part of Innsbruck, Austria, where spring water trickled from Alps limestone rocks and then directly supplied as drinking water without pretreatments. Innsbrucker Kommunalbetriebe (IKB) (https://www.ikb.at/en/) was the water supplier.

Two different types of experimental set-ups were used in this study, a static set-up and a shaking set-up. In all cases treatment and control site had equal temperature, humidity and magnetic background field conditions. The static set-up was designed to represent stagnated water with limited nutrients, and the shaking set-up was designed to represent water under constant mixing and aeration conditions, thus providing a better nutrient/oxygen availability than the static set-up.

2.1. Static set-up

During the experiment, eight beakers (250 mL, 95 × 70 mm) covered with watch glasses (ø 80 mm) were placed either next to a magnet as treated samples or without magnet as control samples. The control samples were placed 5 m away from treated samples to avoid possible interference effects of magnetic fields. The background magnetic fields at the experimental site were measured with a Voltcraft GM-100 Gaussmeter and were <1 G. Polypropylene boxes (395 × 255 × 290 mm) were used to cover the beakers of the control group and treated group separately to provide further protection from contamination (Figure S1d). The static set-up experiment was performed with 8 replicates for each treatment (n = 8 for treated and n = 8 for controls) and has been repeated for 4 times. Only 4 replicates in total were measured for the day 0 samples (original tap water) because the variances among replicates were very small (Figs. 3 and 4).

2.2. Shaking set-up

An orbital shaker was placed on the workbench on both experimental sites which were 5 m apart from each other. Each beaker was magnetically shielded using a special baseplate in order to prevent the magnetic fields generated by the shaker and reduce the magnetic background field to be lower than 1 G (measured with a Voltcraft GM-100 Gaussmeter). These baseplates consisted of a 4 mm thick acrylic plate, a layer of 0.40 mm Mu-Metal sheets, a 12 mm wooden plate, another layer of 0.40 mm Mu-Metal sheets, another 12 mm wooden plate and a final 4 mm acrylic plate (bottom to top). On this baseplate an additional, larger acrylic plate (4 mm) was positioned, on which subsequently up to 24 glass beakers (300 mL, 55 × 95 mm) covered with watch glasses (ø 80 mm) were arranged, with the beakers in the experiment-group being exposed to the magnetic gradients of WCMs. Both treated and control group were covered with a polypropylene box (710 × 440 × 310 mm) and both orbital shakers were operated at 166 RPM. In the treated group, the glass beakers were held in place by two half shells made from PVC water pipes (Figure S2b). In order to test the equivalency of treatment and control site, a double-negative experiment with no WCM present in either group was conducted with the orbital shaker set-up as well. The shaking set-up experiment was repeated three times: two times with 8 replicates ($n = 8$) one time with 24 replicates ($n = 24$). For each repeat, only 4 replicates in total were measured for the day 0 samples (original tap water) because the variances among replicates were very small (Figs. 3 and 4).

For the experiment of *Pseudomonas aeruginosa* in autoclaved drinking water, shaking was also applied. The same tap water used for shaking set-up was collected with a 1 L glass beaker covered with a watch glass, autoclaved for 20 min at 121 °C, then distributed to 16 smaller beakers (100 mL) and *Pseudomonas aeruginosa* (ATCC 27953) culture was added to each beaker resulting in a final concentration of 3 CFU/mL. All operations were performed under sterile conditions in a laminar flow cabinet. Then one half of beakers ($n = 8$) were placed next to the magnet as treated samples and the other half ($n = 8$) were placed 5 m away from the magnet as control samples. The growth of *Pseudomonas aeruginosa* was then monitored over 2–28 days to observe the effect of the treatment on the evolution of cell number at different phases (exponential phase, stationary phase, and death phase).

2.3. Sample preparation

In all cases, the glass beakers were cleaned in a laboratory-dishwasher, and subsequently heat-sterilized for 13 h at 210 °C before use. The water tap was flushed for 20 min before collection of a sample. The water was collected in a 10 L glass beaker and distributed to 48 smaller glass beakers (100 mL each) for further incubation. One half of these beakers were randomly selected and used as control group, the other as the treated group.

2.4. Staining & flow cytometry data analysis

A sample was taken from each beaker at a series of time intervals (every 1 or 2 days) under sterile conditions. Glass beakers from the treated and control group were always handled separately. Staining

procedure followed the protocol described in detail previously (Prest et al., 2013). At each sampling time point, all the incubated water samples from the two conditions, magnetically treated and control, were stained simultaneously. Water samples were first preincubated at 35 °C for 5 min, then 10 μL/mL of a 1:100 dilution of SYBR Green (Sigma-Aldrich S9430) in DMSO were added to 500 μL of water sample, followed by 10 min of incubation at 35 °C in the dark. Subsequently, the samples were put on ice and fixed by formaldehyde (1.4%), and kept in the dark. A maximum number of eight samples were processed in one batch. Flow cytometry data acquisition was done immediately after staining following the procedure described in Prest et al. (2013). Measurements were performed using a BD FACSVerse cytometer (BD Biosciences) equipped with a 20 mW blue laser (488 nm) and with a volumetric counting hardware . Fluorescence intensities at 527 nm ± 32 nm (green fluorescence) and at > 670 nm (far-red) were collected as well as forward- and side scatter signals. A threshold value of 500 was set for the green fluorescence channel. The flow cytometer was calibrated daily according to its manufacturer's standards.

From each sample, data was acquired for 90 s (50 μL/min) and used to extract the total number of microbial cells present in the sample. The gating was calibrated with Milli-Q water, autoclaved tap water, and dilution series to ensure accurate reflection of cell count and identical gating was applied to all the samples. Gated data was then processed with a custom-written R-package (based on the R-packages *flowCore* and *flowWorkspace)* (Ellis et al., 2018; Finak and Jiang, 2011) and presented as a histogram that shows the cumulative cell count at different fluorescent intensity for each water sample. Those histograms were used as fluorescent fingerprint for each water sample. A similar method has been employed before to analyze water from slow sand filters with flow cytometry in drinking water (Prest et al., 2013; Chan et al., 2018) The shaking set-up counts were approximately twice as high as those of the static set-up. Therefore the tail spectra (above 2350) that are not representative of the behavior of the major peaks can have a higher impact on the cell count of the LNA% of the static set-up compared to those of the shaking set-up, a band pass of fluorescent intensity (1600–2350) was applied to allow a more accurate comparison between the static set-up and the shaking set-up (Fig. 1). The threshold to divide LNA from HNA was set differently for each experiment based on evolution of size clustering of cells under the control condition only. Specifically, the cell growth curve was plotted based on the total cell count, then the time point in the beginning of stationary phase was selected and the fluorescent histogram showing the averaged cell count at each fluorescent intensity was plotted. Subsequently, the fluorescent intensity that contained the lowest cell count between two peaks on the fluorescent histogram was determined as the threshold automatically by a custom-written R package (Figure S 3,4). The specific procedure to

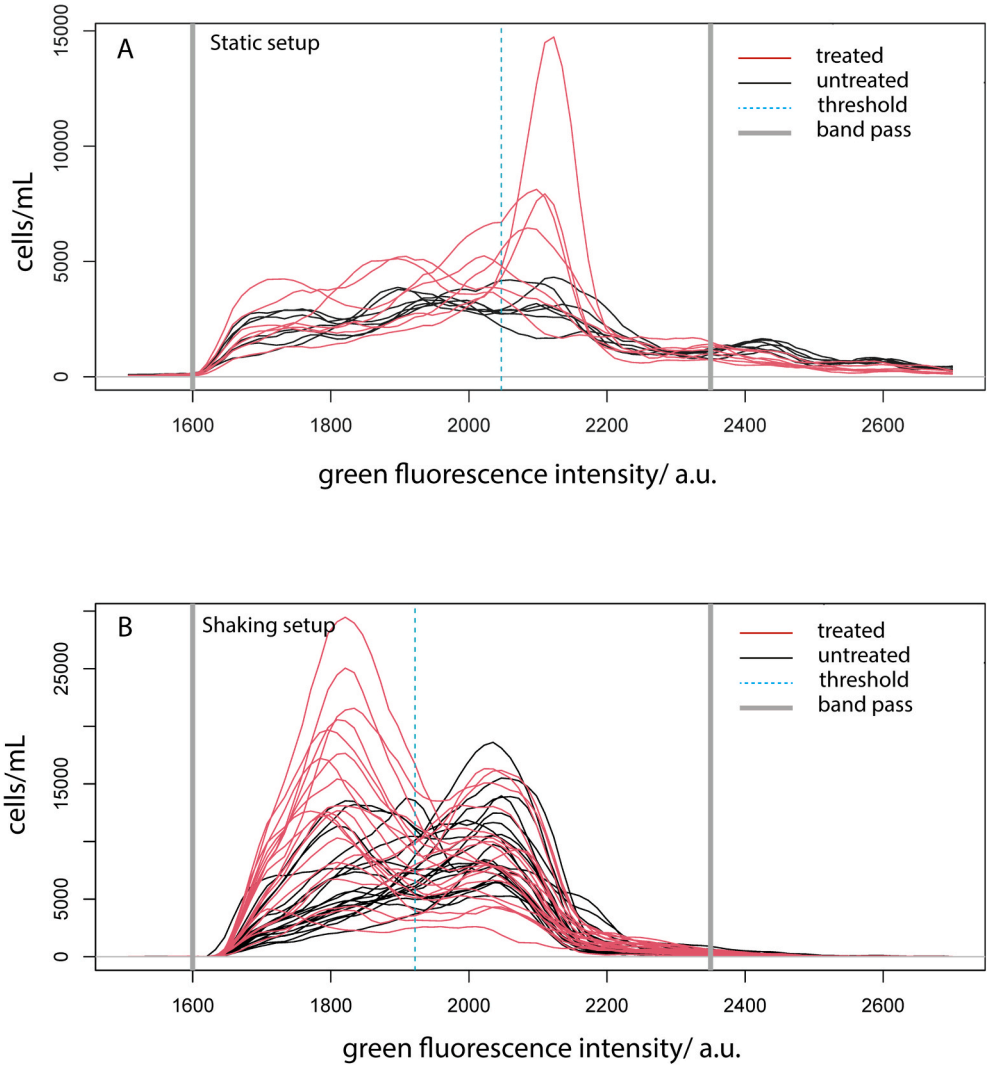

Fig. 1. Distribution of green fluorescence for treatment-group (red) and control-group (black) for A) the static set-up at day 6 and B) the shaking set-up at day 4. The blue dashed line represents the isoemissive region separating cells with high emission intensity from lowly emitting cells (LNA) and was used for the calculation of the percentage of LNA cells. (For interpretation of the references to colour in this figure legend, the reader is referred to the Web version of this article.)

determine the threshold dividing LNA and HNA is listed in Table S4. This method of LNA/HNA gating assumes that LNA and HNA will exhibit different growth behaviors, which will result in development of different amount of nucleic acid content during cell growth in a batch system.

2.5. Statistical evaluation

The experiments with 2 × 24 glass beakers yielded sufficient data to allow an outlier exclusion based on multivariate analysis using the R-packages *aquap2* and *rrcovHD* (Pollner and Kovacs, 2016; Todorov, 2016). This exclusion allows the recognition of both cell count and fluorescence distribution outliers. For experiments with 2 × 8 glass beakers, the outlier exclusion was done based on the number of cells in the group per time point via manual removal of data points outside the whiskers of standard boxplots. After outlier exclusion the data was subjected to standard univariate statistical evaluation (95% confidence interval; all performed in R) (R Core Team, 2017). The data was not normally distributed; therefore the Mann-Whitney-U-tests was applied to test the difference of cell density between the control and magnetically treated samples at each sampling point.

Because the data at each sampling point was not normally distributed, the median (instead of mean) of the total cell concentration, cell concentration of LNA, and cell concentration of HNA at different time points in both static set-up and orbital set-up was used for further growth kinetic analysis. The derived growth curves of LNA and HNA were fitted using a logistic model in the *Growthrates* package in R developed based on the Monod growth model (Kargi, 2009). The maximum growth rate and carrying capacity (maximum population size which can be sustained by a given environment) of total cells, LNA cells, and HNA cells were calculated based on the growth curves using equation (1),

$$y = \frac{K_s \cdot Y_0}{Y_0 + (K_s - Y_0)e^{-\mu_{max} \cdot t}}, \quad (1)$$

where K_s signifies the carrying capacity; Y_0 the initial abundance; μ_{max} the maximum growth rate and t the time.

3. Results

3.1. Observation concerning the flow cytometry data

Fig. 1 represents an example of the fluorescence intensity vs. cell concentration. In general, an effect from the magnetic fields on the cells exhibiting different fluorescence intensity could be observed. Specifically, the number of cells with lower fluorescence intensity increased and the cells with higher fluorescence intensity were inhibited by the magnetic treatment in the shaking set-up whereas in the static set-up, the overall cell density at both lower and higher fluorescence intensity increased. As the fluorescence intensity reflects the nucleic acid content within microbial cells, the amount of stainable nucleic acids in cells may further reflect other characteristics or the behavior of the measured cells. Therefore, quantitative parameters summarizing this observation are needed for further analysis of data. From the evolution of cell densities at different sampling time points, a gradual division of cluster-based fluorescence intensity could be observed along the cell growth. Since such a division was often more evident at the sampling points right before the cell growth entered the stationary phase (around 3–4 days), these sampling points were selected to define the threshold that divided the microbial cells into LNA and HNA. As a result, the threshold was defined individually for each experiment based on the characteristics of fluorescent histograms of each sample during cell growth under untreated condition (Figure S3-4; Table S4). The threshold of all 9 experiments ranged in the middle zone (1850–2050 among 1600–2350) of the fluorescence histogram (Table S2). Subsequently, the final readout of the analysis was reduced to two parameters: the total cell number and the percentage of microbial cells below the threshold as percentage of LNA (%LNA).

3.2. Static set-up

The evolution of total microbial cell numbers and the proportion of LNA/HNA in batch tap water in the static set-up were monitored during 7 days and the effect of the magnetic treatment was evaluated. In general, the increase of total cell concentration follows the general pattern of microbial growth in a batch system, where an exponential growth could be observed in the early phase (day 2–3) and a plateau of cell concentration could be observed in a later phase (day 4–7). The positive effect of the WCM on the total cell number was more distinctive in the second phase (Fig. 2A).

The LNA group has been dominant (>60%) in the control samples during the experiment (Fig. 2B). The %LNA in the treated samples was significantly lower in treated sample for only one day (Fig. 2B) even though the total cells in treated samples were always significantly higher than the one of control samples. It suggested that cell concentrations of both groups were increased by the application of magnetic field (Fig. 2C–D). Specifically, for LNA, even though the maximum growth rate (μmax) of treated cells were slightly lower than untreated cells, the carrying capacity (Ks) increased after the magnetic treatment (Fig. 2C). For HNA cells, the cell growth doesn't fit very well with the logistic growth model for growth rates, but the carrying capacity (Ks) was increased by 50% after magnetic treatment (Fig. 2D). The carrying capacity of HNA was much lower (≈50%) than LNA indicated that under static conditions, the substrate (oxygen) availability is very limited for HNA to achieve a faster growth and higher cell concentration than LNA cells (Table 2). The experiment has been repeated for four times, three showed a significant increase in the total cell concentration (Table 2).

3.3. Shaker set-up

In the shaking set-up a similar general trend like in the static set-up has been observed. The total cell concentration increased exponentially in the first three days and reached the stationary phase from the fourth day on (Fig. 3A). However, the maximum total cell concentration in the shaking set-up in both treated and control samples were higher than the ones in the static set-up, suggesting a better substrate availability and therefore increased carrying capacity of the tap water environment after better mixing (Table 3). Interestingly, the carrying capacity of the same tap water samples increased by more than two-fold after being treated with magnetic fields. At the same time, the %LNA of treated samples (61.79%) was also higher than the %LNA of control samples (43.38%) during the stationary phase, despite the low initial abundance of LNA (13.8%) in both treated and control samples (Fig. 3B).

A closer look at the cell concentration of LNA and HNA separately (Fig. 3C and D) showed that the effect of WCM on LNA was responsible for most of the differences in total cell concentration and %LNA. The tap water's carrying capacity for LNA was improved almost three times after the WCM treatment whereas barely any difference could be observed for HNA after WCM treatment.

The growth rates during the initial stage showed varying dynamics for different microbial groups with or without treatment (Fig. 3C and D). Specifically, on the third day, the total cell concentration (Fig. 3A) was significantly lower in treated samples compared to the control. But this significant difference disappeared immediately in the day afterwards with slightly inverted trend (day 4). Starting from day 5, the cell concentration in treated samples became significantly higher than the one in control samples for five days continuously. The inverted cell concentration between day 3 and day 4 could be explained by the rapid change of growth rate of LNA and HNA under the influence of the magnetic field (Fig. 3C and D). Between day 2 and day 3, in the control group the specific growth rate of LNA (1.88 day $^{-1}$) was higher than the growth rate of HNA (1.54 day $^{-1}$). After day 3, the specific growth rates of all the samples reduced abruptly. For LNA, the specific growth rate

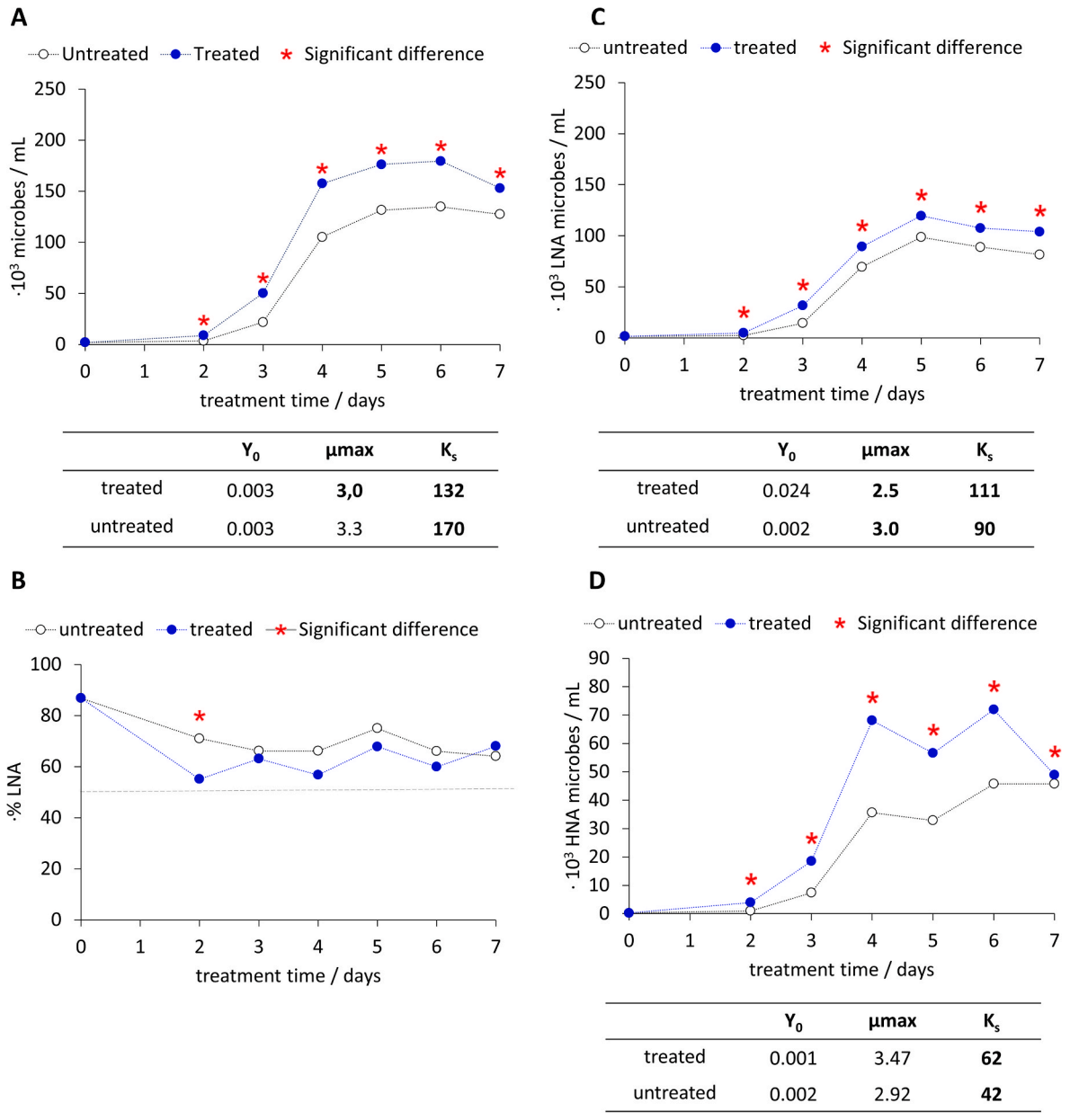

	Y_0	μmax	K_s
treated	0.003	**3,0**	**132**
untreated	0.003	3.3	**170**

	Y_0	μmax	K_s
treated	0.024	**2.5**	**111**
untreated	0.002	**3.0**	**90**

	Y_0	μmax	K_s
treated	0.001	3.47	**62**
untreated	0.002	2.92	**42**

Fig. 2. (A) Median of the total cell concentration and (B) %LNA cells in collected tap water samples over 7 days of incubation time under control (black) condition and WCM treated (blue) condition in the static set-up ($n = 2 \times 8$). Significant differences detected by a Mann-Whitney *U* test are indicated with red stars. (C) Cell concentration of LNA cells and (D) cell concentration of HNA cells at each time point calculated from the median total cell concentration and median %LNA. The cell growth represented by the median of the cell concentration of both HNA and LNA were fitted to a logistic model (Figure S5) and the parameters (initial abundance, Y_0; maximum growth rate, μmax; carrying capacity, Ks) were shown in the table. Only the parameter values that can significantly represents the growth behavior fitting ($p < 0.05$) were shown in bold. Boxplots showing the range of values can be found in figure S6. (For interpretation of the references to colour in this figure legend, the reader is referred to the Web version of this article.)

reduced from 1.88 day $^{-1}$ at day 3 to 0.38 day $^{-1}$ at day 4 in control samples, while in treated samples the growth rate only decreased from 1.67 day $^{-1}$ to 1.54 day $^{-1}$. This effect is possibly due to the increased carrying capacity in the treated samples, which allowed the LNA microbes to maintain a high growth rate. For HNA, the specific growth rate in the treated sample also reduced slower than the control at day 4, however, the difference between treated and control was much smaller compared to LNA. The experiment has been repeated for four times, and all repeats showed an increase in the total cell concentration and/or an increase in the %LNA.

Noticeably, even though the maximum growth rate of HNA was much lower comparing to LNA growth, the estimated starting population at day 2 (Y_0) of HNA was about 500–5000 times higher than LNA. Possibly the maximum growth rate of HNA took place earlier than the sampling point. If we assume the starting population for both LNA and HNA at day 1 was around 10^3 cells/mL, the average growth rate of LNA for the first three days 1.01 day^{-1} will be lower than the ones of HNA (1.17 day^{-1}).

3.4. *Pseudomonas aeruginosa* in autoclaved tap water

To investigate the effect of magnetic treatment on the behavior of a single bacterial species in tap water, *Pseudomonas aeruginosa* was spiked into autoclaved tap water and the evolution of cell number was observed over 28 days. An inhibitory effect of magnetic treatment was observed during the entire growth process, but significant differences could only

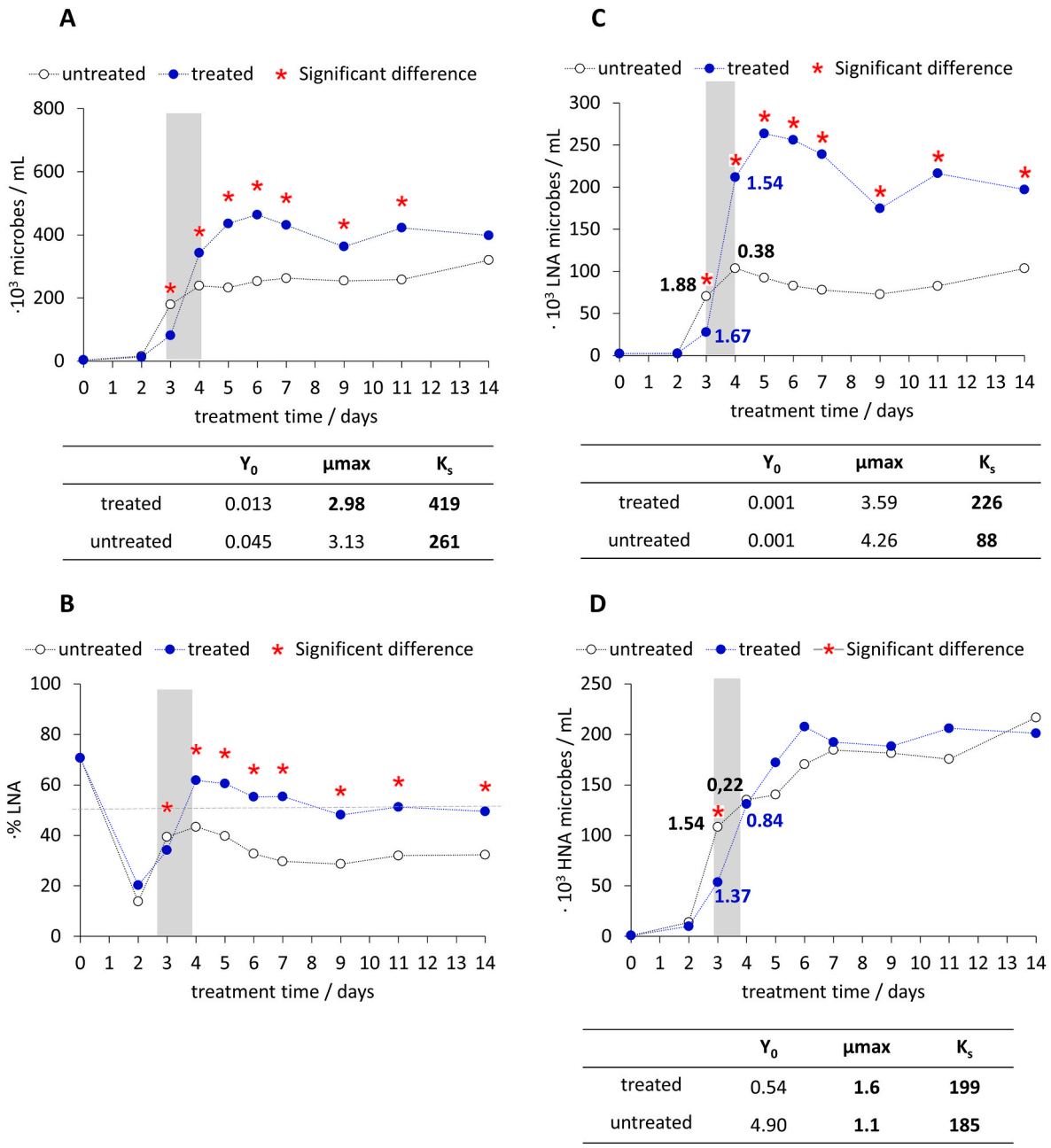

	Y_0	μmax	K_s
treated	0.013	**2.98**	**419**
untreated	0.045	3.13	**261**

	Y_0	μmax	K_s
treated	0.001	3.59	**226**
untreated	0.001	4.26	**88**

	Y_0	μmax	K_s
treated	0.54	**1.6**	**199**
untreated	4.90	**1.1**	**185**

Fig. 3. (A) Median of the total cell concentration and (B) %LNA cells in collected tap water samples during 14 days of incubation time under control (black) condition and WCM treated (blue) condition in the shaking set-up ($n = 2 \times 24$). Significant differences (based on Mann-Whitney U tests) are indicated with red stars. (C) Cell concentration of LNA and (D) cell concentration of HNA at each time point calculated from the median total cell concentration and median %LNA. The numbers in (C) and (D) denote the specific growth rates at day 3 and day 4 (highlighted via vertical light grey bar) in both treated (blue) and control (black) conditions, respectively. The cell growth represented by the median of the cell concentration of both HNA and LNA were fitted to a logistic model (Figure S5) and the parameters (initial abundance, Y_0; maximum growth rate, μmax; carrying capacity, Ks) were shown in the table. Only the parameter values that can significantly represents the growth behavior fitting ($p < 0.05$) were shown in bold. Boxplots showing the range of values can be found in figure S7. (For interpretation of the references to colour in this figure legend, the reader is referred to the Web version of this article.)

be observed at the stationary phase (day 9–21) (Fig. 4), suggesting a reduction of the tap waters carrying capacity for *Pseudomonas aeruginosa* after treatment.

4. Discussion

4.1. r/K framework and cytometric fingerprint

The behavior of HNA and LNA microbes in tap water strongly supports our hypothesis that they represent different microbial groups with different ecological niches and behaviors (Fig. 5). In other words, the different behavior of HNA and LNA microbes at different substrate levels matches fairly well with the r/K strategist model, which states that K-strategists exhibit higher growth rates at lower substrate concentrations and r-strategists exhibit higher growth rates at higher substrate concentrations (Favere et al., 2021; De Vrieze et al., 2017). In detail, under a nutrient limiting conditions (static set-up), the growth rates of LNA microbes were similar to HNA and the carrying capacity (Ks) of the water samples for LNA was approximately twice as high as the one for HNA. But in the shaking set-up where more nutrients and oxygen

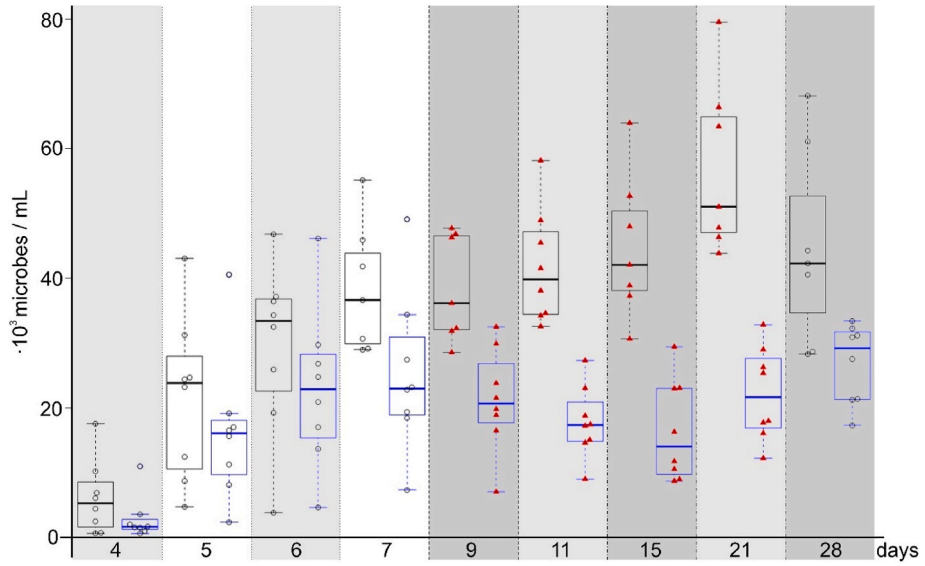

Fig. 4. Cell count of autoclaved tap water spiked with *Pseudomonas aeruginosa* (shaking set-up). WCM treated (blue) and control (black) data is given for day 4 to day 28. Significant differences based on Bonferroni-Holm multiple comparison correction are indicated with red triangles. (For interpretation of the references to colour in this figure legend, the reader is referred to the Web version of this article.)

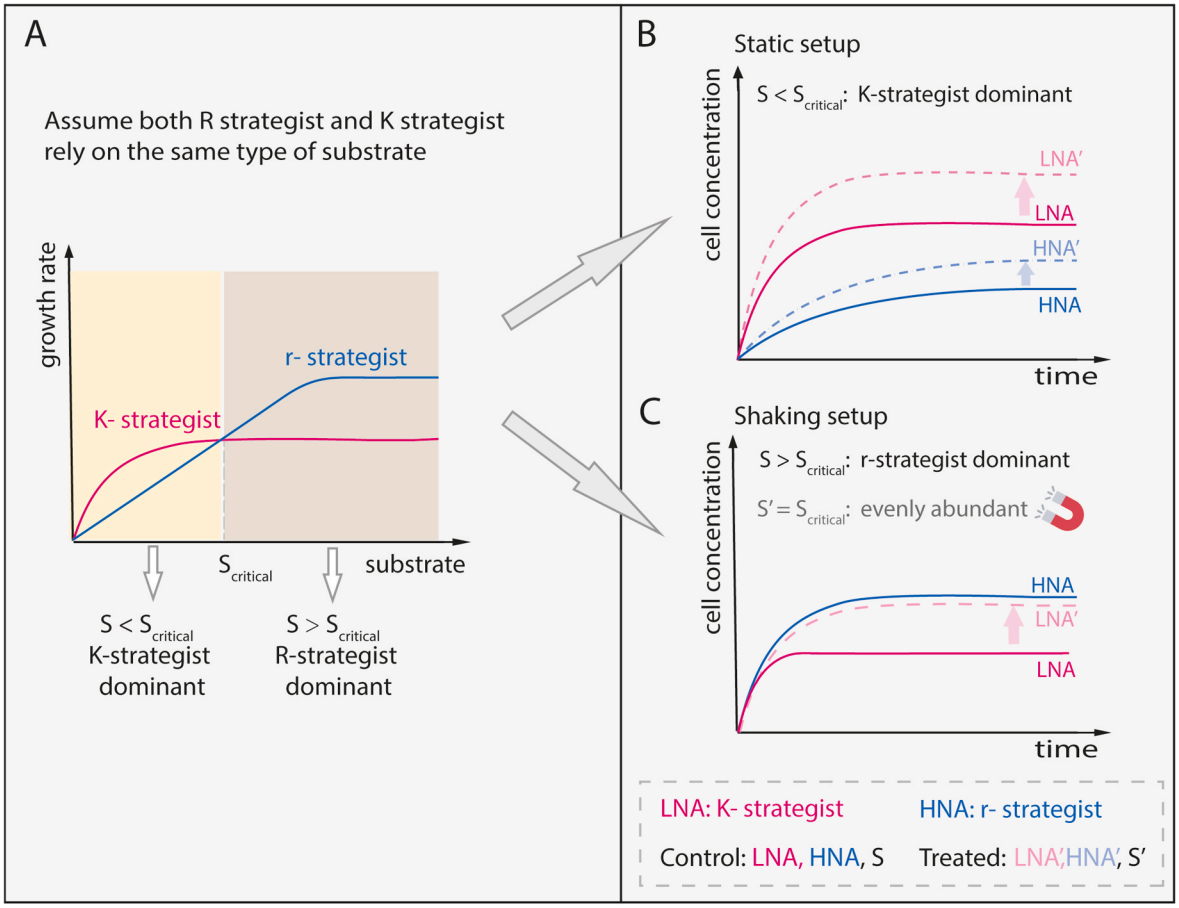

Fig. 5. The growth kinetic of K-strategists and r-strategists at different substrate concentrations. A) The evolution of growth rate of K-strategist and r-strategist at different substrate concentrations. When the substrate concentration S is lower than the critical concentration $S_{critical}$, the K-strategists show higher growth rates. When the substrate concentration S is higher than the critical concentration $S_{critical}$, r-strategists have higher growth rates. B) The growth dynamics in a static set-up: due to the nutrient limitation, K-strategists (LNA) are the dominant group. The WCM treatment increases the growth of LNA and HNA. C) The growth dynamic in a shaking set-up: due to better nutrient availability with the mixing, r-strategists (HNA) are the dominant group. The WCM treatment only increases the growth of LNA but not HNA, therefore the HNA and LNA were evenly abundant after treatment.

became available, the carrying capacity (Ks) of LNA in the control group was approximately half of the one of HNA (Figs. 2B and 3B).

The conceptual framework of r/K strategists has been applied to various microbial processes from hydrocarbon degradation (Brzeszcz et al., 2016), nitrification (Nowka et al., 2015) to methanogenesis (Conklin et al., 2006; De Vrieze et al., 2012). Previous studies, however, are most often based on specific species or genera for a certain functional process. In their extensive literature review, Favere et al. (2021) extended the concept to drinking water ecosystems and proposed that the drinking water microbial communities can also be classified as either r-strategists or K-strategists. To our knowledge, our study is the first experimental study that supports the applicability of this concept on drinking water microbial communities and further shows that by applying flow cytometry method, the r/K strategists are both measurable and manageable. Furthermore, Favere et al. also suggest that a limitation of nutrients should enrich the slow growing non-pathogenic K-strategists and therefore maintain the drinking water at a biostable state, because the enriched K-strategists can exclusively occupy most of the environmental niche that otherwise would have been occupied by r-strategists, who are often pathogens or indicator organisms (Proctor et al., 2018; Ramseier et al., 2011; Rubbens et al., 2019;). This conceptual scenario is also experimentally verified in our study, as the LNA dominated the low nutrient environment leaving the HNA at very low cell concentration. In addition, even though cell growth was observed in the tap water for both static and shaker set-up, the final total cell concentrations in the static set-up were much lower than the ones of the HNA-dominated shaker set-up.

4.2. Effect of magnetic fields on the biostability

Interestingly, the effect of the magnetic field by the WCM treatment acted differently on LNA and HNA microbes in tap water under different conditions. In the static set-up, the maximum growth rate was slightly increased for both LNA and HNA after treatment. In fact, the influence of the magnetic field on the waters carrying capacity was much more striking, as the carrying capacity for LNA was improved by approximately 22% while the one for HNA was increased by about 50%. On the contrary, the enhancive effect of magnetic fields was seen only on LNA in the shaking set-up. In fact, the effect was so pronounced that the community in the tap water shifted from an HNA-dominant structure to an LNA and HNA evenly abundant structure after treatment (Fig. 3B). As no evident effect of magnetic fields on HNA could be observed when using the shaking set-up (Fig. 3D), it seems that the enhancive effect on HNA in the static set-up (Fig. 3D) dependents on the nutrient availability in the system. It was also possible that the LNA cells were promoted by the magnetic field so much that the environmental niche left for HNA became very limited. On the other hand, the inhibitory effect observed on one HNA representative, *Pseudomonas aeruginosa* (Proctor et al., 2018), suggests a potential inhibitory effect of magnetic fields on HNA microbes under nutrient rich condition.

In light of the r/K strategist theory, the selective promotive effect on LNA under nutrient rich conditions can be very beneficial for maintaining the biostability of drinking water. Different studies have suggested a strong correlation between HNA and heterotrophic plate count (HPC) or heterotrophic bacterial production (Lautenschlager et al., 2010; Rubbens et al., 2019), which illustrated the correlation between HNA and pathogens or indicator organisms. Conservatively speaking, it is still unclear whether LNA contain pathogens due to the limited information about the LNA taxonomy (Proctor et al., 2018; Rubbens et al., 2017). The limited number of studies examined taxonomy identification of LNA, however, showed that LNA are mostly associated with oligotrophic, uncultivated bacteria (Nelson and Stegen, 2015; Rubbens et al., 2017, 2019).

In order to determine whether the LNA population consists of smaller HNA cells when there is nutrient shortage, we re-examined the community sequencing data from a previous study which used the same magnetic treatment of stagnant tap water as the static set-up (Paulitsch-Fuchs et al., 2021). This analysis shows an increased diversity and evenness index after magnetic treatment (Figure S8). In addition, the data suggests that most of the bacterial species growing under the influence of the magnetic field were unknown (Figure S8). Both observations support our hypothesis that the LNA species belong to a different bacterial group than the HNA population; and that the growth of this group is selectively enhanced by the magnetic treatment.

In summary, this study illustrated the potential of magnetic treatment to provide a sustainable alternative method for the management of microbial communities in addition to other common methods such as pH, temperature, hydrological regime, or disinfectants (Douterelo et al., 2013; Prest et al., 2016a). To our knowledge, this is the first study to use flow cytometry to illustrate the effect of magnetic fields on drinking water microbial communities.

4.3. Mechanisms behind the selective effect

The categorization of HNA and LNA microbes was based on the fluorescence intensity detected with flow cytometric measurements, which in theory should reflect the nucleic acid content of the microbial cells. The specific relationship between the nucleic acid content and the susceptibility to magnetic fields does not appear to be straightforward. Some elusive clues might be found in a previous study on the functional difference between HNA and LNA cells (Ramseier et al., 2011; Liu et al., 2017). Ramseier et al. (2011) reported that LNA cells in drinking water are much less susceptible to oxidative stresses created by disinfectants (e.g. chlorine) compare to HNA cells, possibly due to different membrane properties of HNA cells. Liu et al. (2017) reported that LNA cells are correlated with metal concentration while HNA cells are not. The difference in membrane structures and the interaction with trace metals might be related to the selectivity of the magnetic influence.

Since the effect of the magnetic field was more pronounced when looking at the carrying capacity instead of at the growth rates, and one of the most important characteristics of K-strategists is their high affinity to nutrients, it is reasonable to speculate that the major influence of magnetic fields on LNA is related to a modified affinity to nutrients. Various previous studies discussed mainly two types of mechanisms of magnetically induced effects: 1) direct effects on biological processes and 2) indirect effects on biological processes through changes in water chemistry (Coey, 2012; Hore, 2012; Liboff, 1985).

Two possible mechanisms employing a direct effect on biological processes are the radical-pair mechanism (Steiner and Ulrich, 1989) and the ion-cyclotron resonance (Liboff, 1985), both have been discussed in our previous work (Paulitsch-Fuchs et al., 2021). The radical-pair mechanism states that the gradient of weak magnetic fields (e.g. earth magnetic field) can affect the quantumly synchronized behavior of the intermediate radical pairs generated during redox reactions and therefore affect the biochemical cascade. More specifically, the electron spins of the radical pair can be flipped by magnetic fields from singlet to triplet state irreversibly, therefore affecting the steps downstream in the biochemical cascade. This mechanism has been studied extensively in the reaction center of photosynthetic bacteria as well as for ATP synthesis in bacteria (Buchachenko et al., 2008; Hore, 2012; Liu et al., 2005). The ATP synthesis studies show that the irreversible spin conversion can push an originally reversible redox reaction towards the oxidative direction, which leads to increased ATP production (Buchachenko et al., 2005).

The other mechanism often discussed is the ion-cyclotron resonance mechanism, which is based on the influence of the Lorentz force on moving charged particles (Goldsworthy et al., 1999; Lednev, 1991; Liboff, 1985). For example, a study by Liboff (1985) showed that even the geomagnetic field intensity could be enough to accelerate the Ca^{2+} flux within helical-shaped transmembrane channels in bacterial or human cells.

Meanwhile, the effects of magnetic fields on water chemistry,

especially calcium carbonate crystallization processes, have been discussed even more often than direct biological effects (Lipus et al., 2015; Baker and Judd, 1996; Knez and Pohar, 2005). One recently discussed mechanism is based on a non-classical nucleation theory stating that calcium carbonate prenucleation clusters (DOLLOPs) exist in undersaturated conditions such as drinking water in addition to the free ions (Bewernitz et al., 2012; Demichelis et al., 2011; Gebauer and Cölfen, 2011). Therefore, the spin conversion induced by magnetic fields on the surface of these prenucleation clusters can affect their size and quantity (Coey, 2012; Sammer et al., 2016). Drinking water bacteria have been reported to intensively interact with calcium and can even participate in calcium carbonate precipitation processes (Liu et al., 2021). In turn, the interaction between calcium and bacterial cells can also be affected (Paulitsch-Fuchs et al., 2021).

A taxonomy study on LNA microbes has indicated a symbiotic lifestyle of LNA due to their small genome and a lack of genes such as for FAD synthase (necessary for nuclear redox activities) or for signal recognition particles (Nelson and Stegen, 2015; Rubbens et al., 2017, 2019). Other studies suggested distinctive membrane properties between LNA and HNA and the dependence of mineral concentrations in water by LNA (Liu et al., 2017; Ramseier et al., 2011). Connecting those scattered pieces of information, we speculate that a combination of both direct and indirect influences that alter the interaction between microbial cells and ions induced by a magnetic field is responsible for the selective effect on LNA cells. More studies will be required for an in-depth understanding.

5. Conclusions

Flow cytometry is a robust method to differentiate functional microbial groups based on nucleic acid content via fluorescence intensities in drinking water. The HNA/LNA microbial groups display distinctive behaviors at different nutrient levels and their behavioral pattern matches well with the prediction from the r/K selection theory. Selective effects of strong gradients in weak magnetic fields of water core magnets on the LNA/HNA groups of tap water could be observed. These results provided strong support to a previously suggested direct biological effect of this treatment (Paulitsch-Fuchs et al., 2021) on tap water next to established physico-chemical effects (Sammer et al., 2016). The effects of the applied magnetic field seem to be beneficial for maintaining biostability of drinking water and have great potential as an alternative tool for microbial management of e.g. drink water supply chains.

Author contribution

Xiaoxia Liu and Bernhard Pollner contributed equally to the presented study. Bernhard Pollner and Xiaoxia Liu planned and performed the experiments. Bernhard Pollner, Nigel P. Dyer, Elmar C. Fuchs and Xiaoxia Liu analyzed the data. Astrid H. Paulitsch-Fuchs provided advise on data analysis. Cornelia Lass-Flörl and Willibald Loiskandl supervised the project. Xiaoxia Liu and Bernhard Pollner wrote the manuscript in consultation with input from Elmar C. Fuchs, Astrid H. Paulitsch-Fuchs, and Nigel P. Dyer.

Declaration of competing interest

The authors declare that they have no known competing financial interests or personal relationships that could have appeared to influence the work reported in this paper.

Acknowledgments

This work was performed in the cooperation framework of Wetsus European Center of Excellence for Sustainable Water Technology (www.wetsus.eu) within the Applied Water Physics theme. Wetsus is cofounded by the Dutch Ministry of Economic Affairs and Ministry of Infrastructure and Environment, The Province of Fryslan and the Northern Netherlands Provinces. The authors thank Pieter van Veelen and Inez Dinkla for fruitful discussions. This research has received funding from the European Union's Horizon 2020 research and innovation programme under the Marie Skłodowska-Curie grant agreement No 665874.

Appendix A. Supplementary data

Supplementary data to this article can be found online at https://doi.org/10.1016/j.envres.2022.113638.

References

Alimi, F., Tlili, M.M., Amor, M. Ben, Maurin, G., Gabrielli, C., 2009. Effect of magnetic water treatment on calcium carbonate precipitation: influence of the pipe material. Chem. Eng. Process. Process Intensif. 48, 1327–1332. https://doi.org/10.1016/j.cep.2009.06.008.

Allen, M.J., Edberg, S.C., Reasoner, D.J., 2004. Heterotrophic plate count bacteria–what is their significance in drinking water? Int. J. Food Microbiol. 92, 265–274.

Baker, J.S., Judd, S.J., 1996. Magnetic amelioration of scale formation. Water Res. 30 (2), 247–260. https://doi.org/10.1016/0043-1354(95)00184-0.

Besmer, M.D., Weissbrodt, D.G., Kratochvil, B.E., Sigrist, J.A., Weyland, M.S., Hammes, F., 2014. The feasibility of automated online flow cytometry for in-situ monitoring of microbial dynamics in aquatic ecosystems. Front. Microbiol. 5, 265.

Bewernitz, M.A., Gebauer, D., Long, J., Cölfen, H., Gower, L.B., 2012. A metastable liquid precursor phase of calcium carbonate and its interactions with polyaspartate. Faraday Dis. 159, 291–312. https://doi.org/10.1039/c2fd20080e.

Brzeszcz, J., Steliga, T., Kapusta, P., Turkiewicz, A., Kaszycki, P., 2016. r-strategist versus K-strategist for the application in bioremediation of hydrocarbon-contaminated soils. Int. Biodeterior. Biodegrad. 106, 41–52. https://doi.org/10.1016/j.ibiod.2015.10.001.

Buchachenko, A.L., Kouznetsov, D.A., Orlova, M.A., Markarian, A.A., 2005. Magnetic isotope effect of magnesium in phosphoglycerate kinase phosphorylation. Proc. Natl. Acad. Sci. U.S.A. 102, 10793–10796. https://doi.org/10.1073/pnas.0504876102.

Buchachenko, A.L., Kouznetsov, D.A., Breslavskaya, N.N., Orlova, M.A., 2008. Magnesium isotope effects in enzymatic phosphorylation. J. Phys. Chem. B 112, 2548–2556. https://doi.org/10.1021/jp710989d.

Chan, S., Pullerits, K., Riechelmann, J., Persson, K.M., Rådström, P., Paul, C.J., 2018. Monitoring biofilm function in new and matured full-scale slow sand filters using flow cytometric histogram image comparison (CHIC). Water Res. 138, 27–36. https://doi.org/10.1016/j.watres.2018.03.032.

Coey, J.M.D., 2012. Magnetic water treatment – how might it work? Philos. Mag. A 92, 3857–3865. https://doi.org/10.1080/14786435.2012.685968.

Conklin, A., Stensel, H.D., Ferguson, J., 2006. Growth kinetics and competition between methanosarcina and methanosaeta in mesophilic anaerobic digestion. Water Environ. Res. 78, 486–496. https://doi.org/10.2175/106143006x95393.

De Vrieze, J., Hennebel, T., Boon, N., Verstraete, W., 2012. Methanosarcina: the rediscovered methanogen for heavy duty biomethanation. Bioresour. Technol. 112, 1–9. https://doi.org/10.1016/j.biortech.2012.02.079.

De Vrieze, J., Christiaens, M.E.R., Verstraete, W., 2017. The microbiome as engineering tool: manufacturing and trading between microorganisms. N. Biotech. 39, 206–214. https://doi.org/10.1016/j.nbt.2017.07.001.

Demichelis, R., Raiteri, P., Gale, J.D., Quigley, D., Gebauer, D., 2011. Stable prenucleation mineral clusters are liquid-like ionic polymers. Nat. Commun. 2, 590–598. https://doi.org/10.1038/ncomms1604.

Douterelo, I., Sharpe, R., Boxall, J., 2013. Influence of hydraulic regimes on bacterial community structure and composition in an experimental drinking water distribution system. Water Res. 47, 503–516. https://doi.org/10.1016/J.WATRES.2012.09.053.

Ellis, B., Haaland, P., Hahne, F., Le Meur, N., Gopalakrishnan, N., Spidlen, J., Jiang, M., 2018. flowCore: Basic Structures for Flow Cytometry Data, version 1.46.1. R-Package.

Favere, J., Barbosa, R.G., Sleutels, T., Verstraete, W., De Gusseme, B., Boon, N., 2021. Safeguarding the microbial water quality from source to tap. NPJ Clean Water 4, 1–6. https://doi.org/10.1038/s41545-021-00118-1.

Finak, G., Jiang, M., 2011. flowWorkspace: Infrastructure for Representing and Interacting with the Gated Cytometry, version 3.28.1. R-Package.

Fojt, L., Strašák, L., Vetterl, V., Šmarda, J., 2004. Comparison of the low-frequency magnetic field effects on bacteria Escherichia coli, Leclercia adecarboxylata and Staphylococcus aureus. In: Bioelectrochemistry, pp. 337–341. https://doi.org/10.1016/j.bioelechem.2003.11.010.

Gabrielli, C., Jaouhari, R., Maurin, G., Keddam, M., 2001. Magnetic water treatment for scale prevention. Water Res. 35, 3249–3259. https://doi.org/10.1016/S0043-1354(01)00010-0.

Gebauer, D., Cölfen, H., 2011. Prenucleation clusters and non-classical nucleation. Nano Today 6, 564–584. https://doi.org/10.1016/j.nantod.2011.10.005.

Goldsworthy, A., Whitney, H., Morris, E., 1999. Biological effects of physically conditioned water. Water Res. 33, 1618–1626. https://doi.org/10.1016/S0043-1354(98)00395-9.

Hammes, F., Egli, T., 2010. Cytometric methods for measuring bacteria in water: advantages, pitfalls and applications. Anal. Bioanal. Chem. 397, 1083–1095. https://doi.org/10.1007/s00216-010-3646-3.
Hore, P.J., 2012. Are biochemical reactions affected by weak magnetic fields? Proc. Natl. Acad. Sci. U.S.A. 109, 1357–1358. https://doi.org/10.1073/pnas.1120531109.
Kargi, F., 2009. Re-interpretation of the logistic equation for batch microbial growth in relationto Monod kinetics. Lett. Appl. Microbiol. 48, 398–401. https://doi.org/10.1111/J.1472-765X.2008.02537.
Knez, S., Pohar, C., 2005. The magnetic field influence on the polymorph composition of CaCO 3 precipitated from carbonized aqueous solutions. J. Colloid Interface Sci. 281, 377–388. https://doi.org/10.1016/j.jcis.2004.08.099.
Lautenschlager, K., Boon, N., Wang, Y., Egli, T., Hammes, F., 2010. Overnight stagnation of drinking water in household taps induces microbial growth and changes in community composition. Water Res. 44 (17), 4868–4877. https://doi.org/10.1016/j.watres.2010.07.032.
Lednev, V.V., 1991. Possible mechanism for the influence of weak magnetic fields on biological systems. Bioelectromagnetics 12, 71–75. https://doi.org/10.1002/bem.2250120202.
Liboff, A.R., 1985. Geomagnetic cyclotron resonance in living cells. J. Biol. Phys. 13, 99–102. https://doi.org/10.1007/BF01878387.
Lipus, L.C., Hamler, A., Ban, I., Acko, B., 2015. Permanent magnets for water-scale prevention. Adv. Prod. Eng. Manag. 10, 209–216. https://doi.org/10.14743/apem2015.4.203.
Liu, Y., Edge, R., Henbest, K., Timmel, C.R., Hore, P.J., Gast, P., 2005. Magnetic field effect on singlet oxygen production in a biochemical system. Chem. Commun. 2, 174–176. https://doi.org/10.1039/B413489C.
Liu, J., Zhao, Z., Chen, C., Cao, P., Wang, Y., 2017. In-situ features of LNA and HNA bacteria in branch ends of drinking water distribution systems. J. Water Supply Res. Technol. - Aqua 66, 300–307. https://doi.org/10.2166/aqua.2017.108.
Liu, X., Zarfel, G., van der Weijden, R., Loiskandl, W., Bitschnau, B., Dinkla, I.J.T., Fuchs, E.C., Paulitsch-Fuchs, A.H., 2021. Density-dependent microbial calcium carbonate precipitation by drinking water bacteria via amino acid metabolism and biosorption. Water Res. 202, 117444 https://doi.org/10.1016/j.watres.2021.117444.
Nelson, W.C., Stegen, J.C., 2015. The reduced genomes of Parcubacteria (OD1) contain signatures of a symbiotic lifestyle. Front. Microbiol. 6, 1–14. https://doi.org/10.3389/fmicb.2015.00713.
Nowka, B., Daims, H., Spieck, E., 2015. Comparison of oxidation kinetics of nitrite-oxidizing bacteria: nitrite availability as a key factor in niche differentiation. Appl. Environ. Microbiol. 81, 745–753. https://doi.org/10.1128/AEM.02734-14.
Paulitsch-Fuchs, A.H., Stanulewicz, N., Dyer, N., Fuchs, E.C., 2021. Strong gradients in weak magnetic fields affect the long-term biological activity of tap water. Water 12, 28–45. https://doi.org/10.14294/WATER.2020.5.
Pinto, A.J., Xi, C., Raskin, L., 2012. Bacterial community structure in the drinking water microbiome is governed by filtration processes. Environ. Sci. Technol. 46 (16), 8851–8859.
Pollner, B., Kovacs, Z., 2016. aquap2: Multivariate Data Analysis Tools for R Including Aquaphotomics Methods. Version 0.3.0, R-Package. In: Kobe, Japan: Aquaphotomics: Understanding Water in Biology - 2nd International Symposium.
Prest, E.I., Hammes, F., Kötzsch, S., van Loosdrecht, M.C.M., Vrouwenvelder, J.S., 2013. Monitoring microbiological changes in drinking water systems using a fast and reproducible flow cytometric method. Water Res. 47, 7131–7142. https://doi.org/10.1016/j.watres.2013.07.051.
Prest, E.I., Weissbrodt, D.G., Hammes, F., van Loosdrecht, M.C.M., Vrouwenvelder, J.S., 2016. Long-term bacterial dynamics in a full-scale drinking water distribution system. PLoS One 11.
Prest, E.I., Hammes, F., van Loosdrecht, M.C.M., Vrouwenvelder, J.S., 2016a. Biological stability of drinking water: controlling factors, methods, and challenges. Front. Microbiol. 7, 1–24. https://doi.org/10.3389/fmicb.2016.00045.
Proctor, C.R., Hammes, F., 2015. Drinking water microbiology-from measurement to management. Curr. Opin. Biotechnol. 33, 87–94. https://doi.org/10.1016/j.copbio.2014.12.014.
Proctor, C.R., Besmer, M.D., Langenegger, T., Beck, K., Walser, J.C., Ackermann, M., Bürgmann, H., Hammes, F., 2018. Phylogenetic clustering of small low nucleic acid-content bacteria across diverse freshwater ecosystems. ISME J. 12, 1344–1359. https://doi.org/10.1038/s41396-018-0070-8.
Props, R., Rubbens, P., Besmer, M., Buysschaert, B., Sigrist, J., Weilenmann, H., et al., 2018. Detection of microbial disturbances in a drinking water microbial community through continuous acquisition and advanced analysis of flow cytometry data. Water Res. 145, 73–82.
Quinn, C.J., Molden, T.C., Sanderson, C.H., 1997. Magnetic treatment of water prevetns mineral build-up. Iron Steel Eng. 47–53.
R Core Team, 2017. R: A Language and Environment for Statistical Computing. R Foundation for Statistical Computing, Vienna, Austria. Retrieved from. https://www.R-project.org/.
Ramseier, M.K., von Gunten, U., Freihofer, P., Hammes, F., 2011. Kinetics of membrane damage to high and low nucleic acid bacterial clusters in drinking water by ozone, chlorine, chlorine dioxide, monochloramine, ferrate-VI, and permanganate. Water Res. 45, 1490–1500. https://doi.org/10.1016/j.watres.2010.11.016.
Reasoner, D.J., Geldreich, E.E., 1985. A new medium for the enumeration and subculture of bacteria from potable water. Appl. Environ. Microbiol. 49, 1–7.
Rubbens, P., Props, R., Boon, N., Waegeman, W., 2017. Flow cytometric single-cell identification of populations in synthetic bacterial communities. PLoS One 12, 1–19. https://doi.org/10.1371/journal.pone.0169754.
Rubbens, P., Schmidt, M.L., Props, R., Biddanda, B.A., Boon, N., Waegeman, W., Denef, V.J., 2019. Randomized lasso links microbial taxa with aquatic functional groups inferred from flow cytometry. mSystems 4, 1–17. https://doi.org/10.1128/msystems.00093-19.
Sammer, M., Kamp, C., Paulitsch-Fuchs, A.H., Wexler, A.D., Buisman, C.J.N., Fuchs, E.C., 2016. Strong gradients in weak magnetic fields induce DOLLOP formation in tap water. Water 8. https://doi.org/10.3390/w8030079.
Segatore, B., Setacci, D., Bennato, F., Cardigno, R., Amicosante, G., Iorio, R., 2012. Evaluations of the effects of extremely low-frequency electromagnetic fields on growth and antibiotic susceptibility of Escherichia coli and Pseudomonas aeruginosa. Internet J. Microbiol., 587293 https://doi.org/10.1155/2012/587293, 2012.
Šolić, M., Krstulović, N., Vilibić, I., Bojanić, N., Kušpilić, G., Šestanović, S., Šantić, D., Ordulj, M., 2010. Variability in the bottom-up and top-down controls of bacteria on trophic and temporal scales in the middle Adriatic Sea. Aquat. Microb. Ecol. 58, 15–29. https://doi.org/10.3354/ame01342.
Steiner, U.E., Ulrich, T., 1989. Magnetic field effects in chemical kinetics and related phenomena. Chem. Rev. 89, 51–147.
Strašák, L., Vetterl, V., Šmarda, J., 2002. Effects of low-frequency magnetic fields on bacteria Escherichia coli. Bioelectrochemistry 55 (1–2), 161–164. https://doi.org/10.1016/S1567-5394(01)00152-9.
Taguer, M., Quillier, O., Maurice, C.F., 2021. Effects of oxygen exposure on relative nucleic acid content and membrane integrity in the human gut microbiota. PeerJ 9. https://doi.org/10.7717/peerj.10602.
Todorov, V., 2016. rrcovHD: Robust Multivariate Methods for High Dimensional Data, version 0.2-5, R-package. Retrieved from. https://CRAN.R-project.org/package=rrcovHD.
Van Nevel, S., De Roy, K., Boon, N., 2013. Bacterial invasion potential in water is determined by nutrient availability and the indigenous community. FEMS Microbiol. Ecol. 85, 593–603. https://doi.org/10.1111/1574-6941.12145.
Van Nevel, S., Buysschaert, B., De Gusseme, B., Boon, N., 2016. Flow cytometric examination of bacterial growth in a local drinking water network. Water Environ. J. 30 (1–2), 167–176.
Van Nevel, S., Koetzsch, S., Proctor, C.R., Besmer, M.D., Prest, E.I., Vrouwenvelder, J.S., et al., 2017. Flow cytometric bacterial cell counts challenge conventional heterotrophic plate counts for routine microbiological drinking water monitoring. Water Res. 113, 191–206.
Vermeiren, T., 1958. Magnetic treatment of liquids for scale and corrosion prevention. Corr. Techn. 5, 215–219.
Wang, Y., Hammes, F., De Roy, K., Verstraete, W., Boon, N., 2010. Past, present and future applications of flow cytometry in aquatic microbiology. Trends Biotechnol. 28, 416–424.